Bathymetric mapping by means of remote sensing: methods, accuracy and limitations

Jay Gao*

School of Geography, Geology and Environmental Science, The University of Auckland, Private Bag 92019, Auckland, New Zealand

Abstract: Bathymetry has been traditionally charted *via* shipboard echo sounding. Although able to generate accurate depth measurements at points or along transects, this method is constrained by its high operating cost, inefficiency, and inapplicability to shallow waters. By comparison, remote sensing methods offer more flexible, efficient and cost-effective means of mapping bathymetry over broad areas. Remote sensing of bathymetry falls into two broad categories: non-imaging and imaging methods. The non-imaging method (as typified by LiDAR) is able to produce accurate bathymetric information over clear waters at a depth up to 70 m. However, this method is limited by the coarse bathymetric sampling interval and high cost. The imaging method can be implemented either analytically or empirically, or by a combination of both. Analytical or semi-analytical implementation is based on the manner of light transmission in water. It requires inputs of a number of parameters related to the properties of the atmosphere, water column, and bottom material. Thus, it is rather complex and difficult to use. By comparison, empirical implementation is much simpler and requires the input of fewer parameters. Both implementations can produce fine-detailed bathymetric maps over extensive turbid coastal and inland lake waters quickly, even though concurrent depth samples are essential. The detectable depth is usually limited to 20 m. The accuracy of the retrieved bathymetry varies with water depth, with the accuracy substantially lower at a depth beyond 12 m. Other influential factors include water turbidity and bottom materials, as well as image properties.

Key words: analytical method, bathymetric mapping, empirical modelling, LiDAR, remote sensing.

I Introduction

Accurate determination of water depth is important both for the purposes of monitoring underwater topography and movement of deposited sediments, and for producing nautical charts in support of navigation. Such information is also critical to port facility management, dredging operations, and to predicting channel infill and sediment budgets. Bathymetry has been conventionally

*Email: jg.gao@auckland.ac.nz

mapped using vessel-based acoustic echo sounding. This method is able to generate accurate point measurements or depth profiles along transects, but is constrained by inefficiency, expense and inaccessibility. Environmental conditions and technological restraints prevent its applicability to nearshore waters (Tronvig, 2005) as shallow coastal waters are hazardous to navigate, especially at low tides. An alternative is to combine shipboard and satellite data to improve bathymetric prediction (Sichoix and Bonneville, 1996). In this 2-D spectral method, bathymetry is predicted from a compensation model with two layers for the crust. This method is disadvantaged by its coarse horizontal resolution of 8 km and poor accuracy of <300 m. By comparison, the remote sensing method is faster and applicable to various environments, including shallow coastal waters, clear rivers, and the relatively clean riverine reaches in the upper parts of estuaries (Roberts and Anderson, 1999).

Remote sensing of bathymetry takes several forms, each having its own detection depth, accuracy, strengths, limitations and best application settings. These forms fall into two broad categories: non-imaging and imaging (Table 1). The non-imaging method as exemplified by light detection and ranging (LiDAR) detects the distance between the sensor and the water surface/sea floor using a single wave or double waves. It is the lapse of the returned radiation pulses from the target at the sensed spots that are used to generate bathymetric information. By comparison, imaging methods base the estimation of water depth on the pixel values of an image. They make use of the visible light and microwave radiation. On microwave imagery, radar backscatter captures variations in sea surface roughness that are caused by modulations in the wave spectrum related to surface current velocity (Vogelzang *et al.*, 1992). Variations in the current velocity at the sea surface manifest interactions between tidal flow and bottom topography. Although this method is not subject to cloud cover, it is rather complex as numerical instead of analytical inversion is used to derive bathymetry from speckle-infested radar imagery (Calkoen *et al.*, 2001). In addition, its accuracy is rather low as a result of its vulnerability to wind influences (Table 1). Consequently, it has found limited applications in shallow seas and open waters, and will not be covered further in this paper.

Unlike microwave sensing, optical imaging is able to determine water depth directly from the radiometric properties of the captured image. One particular form of the imaging methods is video imaging that provides continuous data recording automatically in nearshore waters (Aarninkhof *et al.*, 2003). It is best deployed in the intertidal zone to map beach bathymetry, and to survey shoreline elevations less than 15 cm. A successful example of the video-based method is the subtidal beach mapper method for estimating nearshore bathymetry (Aarninkhof *et al.*, 2005). As such, it is incapable of applications in offshore waters (Table 1). A variant of this method is remote sensing imagery integrated with open-channel flow principles (Fonstad and Marcus, 2005). Such a hydraulically assisted bathymetry technique is suitable for estimating the depth of rivers without the need for *in situ* depth information at the time of flight.

Airborne optical sensing of bathymetry is by far the most frequently used for a wide range of water bodies, including inland lakes, shallow estuaries, coastal areas, and open seas. This method can be implemented either analytically or empirically. Each implementation has its own strengths and limitations. The purpose of this paper is to provide a comprehensive evaluation of the two broad categories of non-imaging and imaging methods of bathymetric mapping, including the principles underlying each method. It particular, this paper concentrates on the retrieval of water depth by means of optical remote sensing both analytically and empirically, and the influence of a variety of factors, including

Table 1 Comparison of non-imaging and imaging methods for bathymetric mapping

Method	System	Sensible depth	Accuracy	Affecting factors	Strengths	Limitations	Best use
Non-imaging	LiDAR	Up to 70 m	Up to 15 cm	Water clarity, bottom material, surface state, background light	Wide depth range; concurrent measurement not essential	Expensive Limited swath width	Diverse environments of a narrow range (eg, tens of km wide)
Imaging	Microwave (space-borne)	Shallow to deep	Low	Image resolution slicks, fronts, weather condition (eg, waves)	Over large areas Not subject to cloud cover	Not so accurate	Open oceanic waters
Imaging	Optical – analytical	Up to 30 m	High	Water quality, atmospheric conditions	Based on physical process Accurate	Complex as several input parameters required Concurrent sea truth essential	Turbid and shallow inland waters, estuaries and river channels
Imaging	Optical – empirical	Up to 30 m	Varying	Atmospheric calibration, water turbidity Bottom reflectance	Simple to implement Accurate at certain depth	Limited depth Accuracy lower at a larger depth Concurrent sea truth essential	Nearshore and coastal waters; open waters
Imaging	Video	Tidal height	High	Image resolution	Able to reveal minor bathymetric change	Restrictive area Bathymetry along profiles	Intertidal zone and estuaries

water quality, on the accuracy and range of retrievable water depth. Each method of depth retrieval is evaluated for its accuracy, detectable depth, best application situations and limitations.

This paper is organized into six parts. After this introduction, the non-imaging method is presented first. Next, the two means of implementing the optical method are presented and compared with each other. Then, the empirical modelling method is described and the factors related to its performance are reviewed. Following this, the paper concentrates on the accuracy of the retrieved bathymetry and the water quality parameters that affect the accuracy of depth retrieval. Finally, this paper ends with a summary and conclusions.

II Non-imaging bathymetric mapping
Bathymetric mapping using the non-imaging method is exemplified by airborne LiDAR (light detection and ranging). Also known as optical radar or laser radar, LiDAR transmits high-power pulses of laser light at short intervals over an area and receives the signal returned from the sensed surface. Water depth is measured from the two-way travel time of a pulse between the water surface and the sea floor. After the surface-reflected and floor-reflected pulses are identified, water depth is calculated from the time difference between the two pulses.

Detection of the water surface and the sea bottom, and determination of the distance between them require recording of the entire temporal sequence of the LiDAR return through the water column (the waveform) in a one-beam system. This waveform contains vital information on the propagation of LiDAR pulses at different depths and over different bottom materials. A generic waveform (Figure 1) comprises three components: surface return, water column backscattering and bottom return. The first is usually the strongest, but can be quite variable with surface conditions. It can disappear altogether over a flat surface as a consequence of specular reflection. On the other hand, surface waves complicate the use of the bottom return signal by exaggerating the value and variance of its amplitude. Water volume backscattering begins as the pulse strikes the water surface, and increases until it is entirely submerged in the water. In this case, the backscattering is exponentially attenuated with respect to the product of water depth and the diffuse coefficient (Wang and Philpot, 2007). The bottom return is the last signal to reach the sensor. Due to the aforementioned reasons, this component is typically many orders lower than the surface return in magnitude. In order to maximize the depth of penetration, bathymetric LiDAR usually makes use of the green laser light. Longer wavelength radiation is not favoured due to increasing absorption by water. Shorter wavelengths are not ideal either because of strong scattering and absorption by in-water constituents, and hence a shallower depth of penetration (Wang and Philpot, 2007). For coastal waters, the deepest penetration takes place at the blue-green wavelength of 540 nm. Alternatively, a LiDAR system may make use of two beams, one green beam (532 nm) for penetration through the water, and one infrared beam for determining the range between the sensor and the water surface. Bathymetry is derived from the maxima of the two main signals (Mallet and Bretar, 2009).

The feasibility of estimating water depths using airborne pulsed blue-green laser was demonstrated as early as the late 1960s (Hickman and Hogg, 1969). The use of LiDAR in shallow water bathymetry was pioneered by Lyzenga (1985). However, it did not find wide applications until the advent of the global positioning system (GPS). A GPS-capable LiDAR system allows the measurement of sea bottom without concurrently measuring water-level data, while avoiding errors caused by highly dynamic temporal and spatial water-level variations. It is able to perform fast,
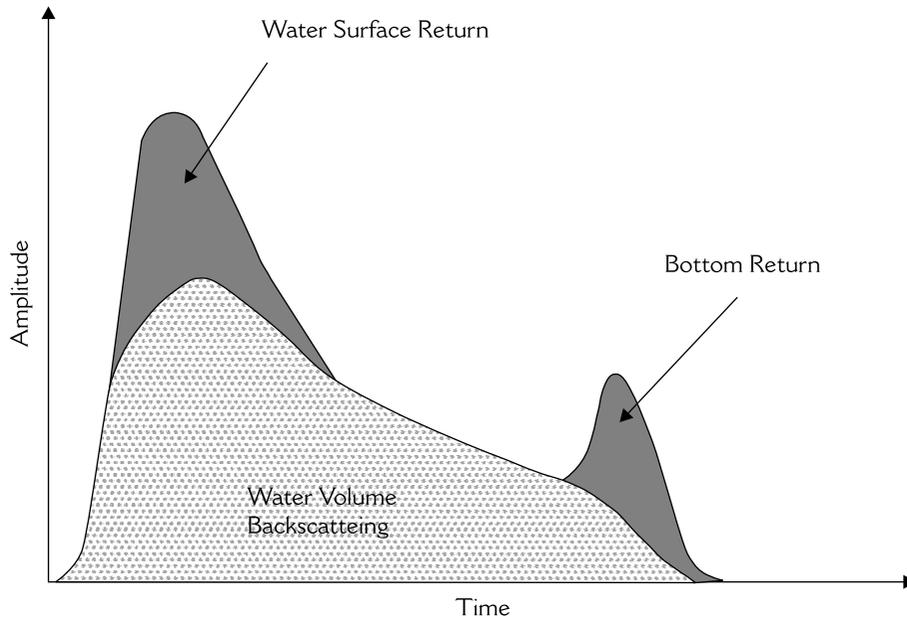
Figure 1   Generic bathymetric LiDAR waveform
Source: Wang and Philpot (2007).

accurate and cost-effective bathymetric surveys of navigation channels, coastal structures, large offshore areas, beaches and shorelines. If a LiDAR system is augmented with the ability to utilize kinematic GPS with on-the-fly phase ambiguity resolution, a vertical reference can be established at sub-decimetre accuracy (Guenther *et al*., 2000).

Airborne LiDAR holds great promise for mapping seafloor topography in coastal waters that have low suspended sediment concentrations or are not discoloured by organic pigments (Finkl *et al*., 2005). A large volume of high-quality data can be acquired efficiently *via* variable swath widths independent of water depth. LiDAR is capable of measuring water depth from 1.5 to 60 m (Abbot *et al*., 1996) at an accuracy level of up to 15 cm. The maximum depth of penetration ranges from 35 m to 50 m. Limiting factors are identified as water clarity, bottom material and composition, weather and sea state, background light and eye safety

(Muirhead and Cracknell, 1986). LiDAR is most suited for clear Case II waters in which it is able to map bathymetry up to 70 m deep, or about two to three times the Secchi depth. A generally accepted wind speed limit which allows full use of the system appears to be 10 m/s (20 knots) and wave heights should be less than 1 m. A distinct advantage of LiDAR is the redundancy of the need for concurrently acquired sea-truth bathymetric data (Table 1). However, this method is limited by its expense and a narrow range of swath, but these may be overcome with the advent of space-borne LiDAR in the future.

III Optical sensing of bathymetry
Optical bathymetry is underpinned by the principle that the total amount of radiative energy reflected from a water column is a function of water depth. It takes advantage of shortwave radiation in the blue and green spectrum that has a strong penetration capability. As the incident solar radiation

propagates through the water, it is increasingly scattered and absorbed by water and in-water constituents, leaving varied energy to be backscattered and recorded in remote sensing imagery. The energy received at the sensor is inversely proportional to the depth of water after atmospheric and water column effects have been removed. Therefore, the intensity of the returned signal is indicative of the depth at which the solar radiation has penetrated. Optical sensing of bathymetry, also known as passive remote sensing, requires a model between radiance values on satellite imagery and the depths at sampled locations. This model can be analytical, semi-analytical or empirical.

1 Analytical modelling

Analytical modelling of bathymetry is based on the manner of light propagation in water. The establishment of this model requires the input of a number of optical properties of water, such as the attenuation coefficient and backscattering. The commonly used model is the flow radiative transfer model which requires the input of the spectral signatures of suspended and dissolved materials, and bottom reflectance $R_b(\lambda)$ (Spitzer and Dirks, 1986). According to this model, water column depth D is calculated as:

$$D = \frac{1}{Kf} Ln(\frac{C \bullet R_b(\lambda)}{L - L_\infty})$$ (1)

where K stands for the effective attenuation coefficient of the water; f is a geometric factor accounting for path length; L refers to the radiance value of a spectral band; L_∞ is the mean radiance over deep water caused by water surface reflection, water column, and atmospheric scattering; C is a constant derived from irradiance at the sea surface, the transmittance of the sea surface and the atmosphere, and the reduction of the radiance due to refraction at the sea surface.

The radiative transfer model involves the inherent assumption of a highly reflective bottom, an appropriate level of water quality, and/or shallow depth. It is inapplicable to coastal waters that have a poor reflecting bottom due to high turbidity. Thus, it needs modification in turbid waters in which bottom reflection is disguised or in deep waters where bottom reflection does not exist. In such environments the model proposed by Ji *et al.* (1992) is more suitable:

$$D = -\frac{1}{K} Ln(1 - \frac{L - B'}{A'})$$ (2)

where A' is a parameter related to atmospheric transmission and the irradiance reflectance of an optically deep water column; B' contains only atmospheric and sky irradiance effects; Both are determined through regression analysis based on sea-truth bathymetric data. With some modification this model can be applied to very shallow (eg, $D < 2$ m) waters.

Similarly, the Benny and Dawson (1983) model is also applicable to shallow waters:

$$D = \frac{Ln(L_x - L_d) - Ln(L_o - L_d)}{-K[1 + \cos(E')]}$$ (3)

where L_d and L_o refer to the radiance from deep and shallow waters, respectively. These are determined from the histogram of pixel values for the water area. The reflectance value from the left tail of the histogram is taken to be an estimate of L_d while that from the upper part is taken as an estimate of L_o (Muslim and Foody, 2008); L_x stands for the radiance from water of depth x, and E' is the incident angle of incoming radiation with respect to the water surface. This model takes into account the attenuation of the reflected light from the bottom by using points with known depths. Hence, the local setting is considered in estimating K. This value performs a type of calibration on the satellite data and relates it to the actual water surface conditions. This algorithm is recommended for use after integrating local conditions into their structure (Baban, 1993).

In areas of homogeneous water optical properties and a uniform bottom type, the estimation of water column depth D may

take advantage of the modified and rescaled model by Philpot (1989):

$$D = -\frac{1}{g} Ln(\frac{L_d - L_o}{L_b}) \qquad (4)$$

where g is an effective attenuation coefficient of the water; L_d stands for the remotely sensed radiance over optically deep water (eg, $D \rightarrow$ infinity); L_b is a radiance term sensitive to bottom reflectance. Apart from the histogram method, L_o can also be determined through the darkest pixel method. In implementing this model, digital count values instead of radiances may be used.

All the above models are common in that they involve the use of a single band while the rich information in other multi-spectral bands is wasted. This limitation in estimating bathymetry is overcome by the simple physically based algorithm proposed by Lyzenga *et al*. (2006):

$$D = -\frac{1}{\alpha} [Ln(L_b) - Ln(L' - L_s')] \qquad (5)$$

where α represents the sum of the diffuse attenuation coefficients for upwelling and downwelling light; L_b includes the transmission losses through the air-water interface, and bottom reflectance and volume-scattering effects; L' stands for the radiance corrected for sun glint and/or atmospheric variations; L_s' is the average return from deep water that has been corrected for sun glint, but still subject to the column scattering effect. This model is applicable to areas of uniform water optical properties and bottom reflectance. In contrast to the previous models, it takes into account the sun glint. In addition, it involves the use of multi-spectral bands that can effectively suppress errors in water depth estimates caused by variations in bottom reflectance and/or water optical properties.

2 Empirical modelling

In empirical modelling, the relationship between the remotely sensed radiance of a water body and the depth at sampled locations is established empirically without regard to how light is transmitted in water. A close relationship exists between water depth and the radiance of a single band for waters of uniform optical properties and bottom reflectance. If the optical properties are not uniform, multiple bands must be used (Lyzenga, 1978). The development of this empirical model requires a set of *in situ* measurements that may encompass water reflectance and bottom reflectance, the vertically averaged diffuse attenuation coefficient, and the concentrations of suspended inorganic constituents, chlorophyll a, pheopigments and dissolved organic carbon (Lafon *et al*., 1997). The field measured spectral reflectance over a wide range of wavelength should reveal the most suitable band(s) for sensing bathymetry. This is especially important in conditions of spatially varying turbidities. Other *in situ* measurements may include collection of water samples using bottles, and determination of water depth at the sampling spots using a sound echoer. Their coordinates in a geographic reference system are determined using a GPS (Figure 2).

The establishment of this empirical model is *via* least squares regression analysis. Regression of the observed water depth against the spectral reflectance in the most sensitive spectral band(s) is able to yield an empirical model for water depth. Application of this model to the entire image leads to the generation of a bathymetric map. The empirical modelling method is valid given that the total water reflectance is related primarily to water depth, and secondarily to water turbidity (Lafon *et al*., 2002). This claim has been backed by Ji *et al*. (1992) who concluded that water column scattering dominates the exit radiance from water unless it is very shallow and transparent or overlies a highly reflective bottom.

3 Comparison of methods

Both implementations of the optical method are very efficient for mapping bathymetry over a large area. They are able to yield finer
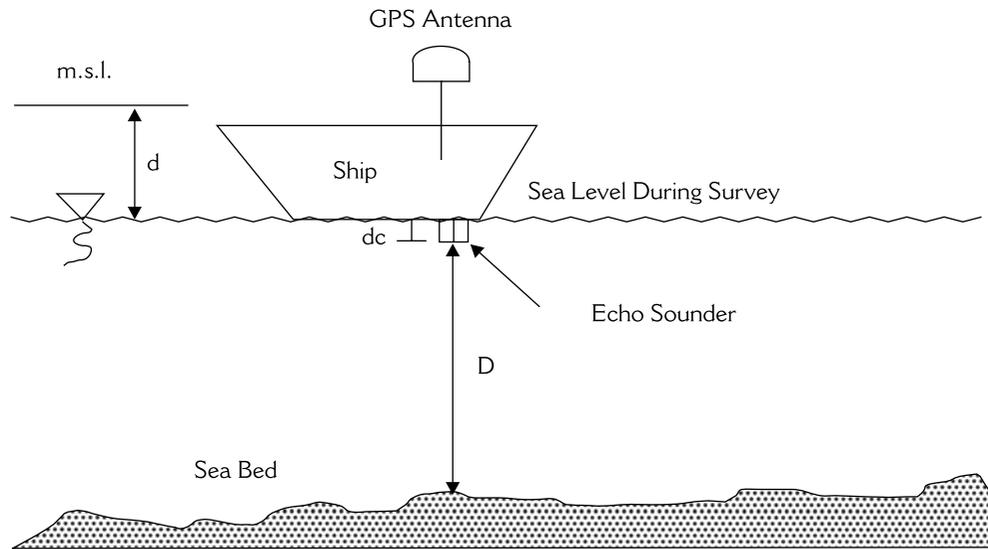
Figure 2   Collection of *in situ* water depth using a GPS-enabled echo sounder in constructing the estimation model

Source: modified from Tripathi and Rao (2002).

resolution depth information than the LiDAR method, even though the range of detectable depths is reduced. Under optimum conditions, the discernible depth rarely exceeds 20 m and uncertainties can be worse than 4–5 m (Muirhead and Cracknell, 1986). Usually, sea-truth data must be collected concurrently for model construction. Both types of methods are limited in that it is very difficult to calibrate the detected depth.

All analytical models require radiometric calibration to account for the atmospheric effect irrespective of their specific format (Table 1). The analytical implementation is more accurate, but very complex, and requires the input of more parameters related to the water and even the atmosphere. Thus, it is highly complicated, but can yield highly accurate bathymetric information. By comparison, empirical modelling is much simpler and easy to use. This regression-based model is able to take into account the local set of conditions of the study area, and the atmospheric effects on the electromagnetic waves path in its structure (Baban, 1993). Therefore,

it is not always vital to calibrate the remote sensing imagery radiometrically.

IV Empirical modelling of bathymetry
The actual estimation of bathymetry based on empirical modelling requires proper selection of the sensing wavelength band(s), and model construction and validation.

1 Selection of optimal spectrum
The selection of the best spectral bands is governed by their capability in penetrating water, and the aquatic environment. Theoretically, the blue spectrum (0.45–0.52 μm) should be selected for optically sensing bathymetry due to its strong penetration capabilities. Spectral bands of short wavelengths are preferred in bathymetric mapping from space as there is low attenuation of electromagnetic radiation. For instance, the maximum penetration for the multi-spectral scanner (MSS) 4 (0.4–0.5 μm) is as deep as 25 m, but only 6 m for MSS 5 (0.5–0.6 μm) (Polcyn and Lyzenga, 1979). Band 1 (0.52–0.59 μm) of LISS III has the closest
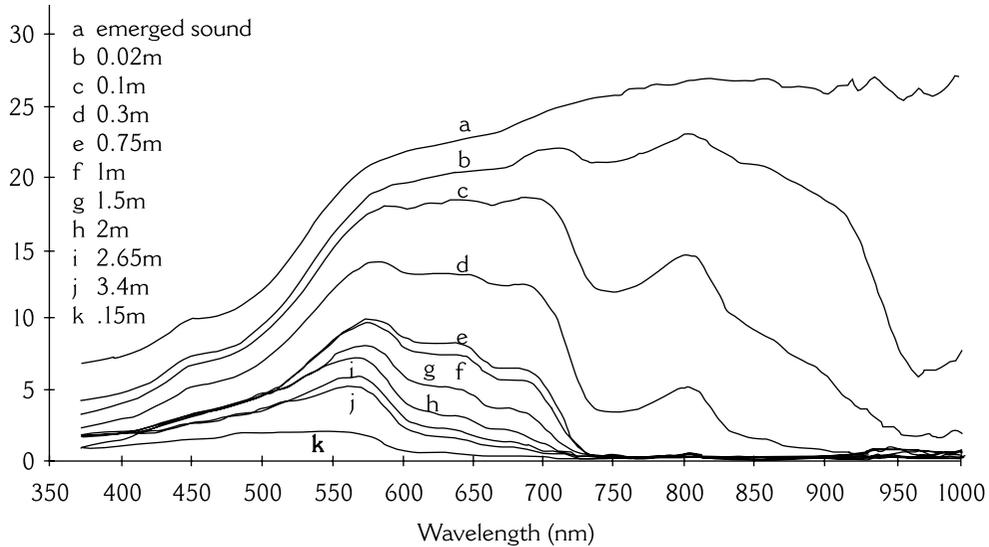
Figure 3 Reflectance spectra of water at depths ranging from 0.02 to 15 m
Source: adapted from Lafon *et al.* (2002).

correlation of 0.978 with corrected water depth among all bands (Tripathi and Rao, 2002). However, this spectrum has not been universally accepted as the optimal. The optimal wavelength ranges for an estuary are 0.5–0.6 μm (Warne, 1972) and 0.77–0.80 μm (Kumar *et al.*, 1997).

The varied optimal wavelengths are explained by water clarity and the sensing environments. In pure and clear waters, little backscattering takes place and radiation is able to penetrate the deeper water. Nevertheless, the short wavelength algorithms advocated for bathymetric measurements in clear water cannot be applied to turbid productive waters. Turbid waters shift the optimum wavelength of sensing bathymetry towards longer radiation, away from the vicinity of 0.45 μm that tends to have the maximum penetration in clear waters (Siegal and Gillespie, 1980). In this environment, water depth is strongly correlated with the red band of the 0.746–0.759 μm range, but not the blue end of the spectrum (George, 1997). The best way of determining the optimal wavelength for a water body is to

measure the spectrum at different depths and select the wavelength ranges most sensitive to bathymetry (Figure 3).

2 Model construction
The simplest regression model for water depth D takes the following form:

$$D = A + B \times R \qquad (6)$$

where A and B are regression coefficients and R is the spectral reflectance in a band or a ratio derived from multiple bands. The existence of this linear relationship for water depth up to 40 m has been confirmed for the waters in Penang, Malaysia (Ibrahim and Cracknell, 1990), and between water depth and IRS-1D linear independent self-scanner III band 1 data (Tripathi and Rao, 2002). Satisfactory results have been obtained with single-band measurements of absolute radiance, multi-band algorithms or measurements of relative radiance in deep and shallow water (Benny and Dawson, 1983). In the case of a pair of bands, their ratio is able to eliminate the impact of bottom reflectance that is thought

to be consistent at different wavelengths (Dierssen *et al*., 2003).

Apart from the linear model, non-linear and exponential models have also been used – for instance, the second-order polynomial equation by Dierssen *et al*. (2003). It is also common to transform depth using natural logarithms before the results are regressed against individual spectral bands (Baban, 1993). Accurate depth estimates can be derived by using transformed input brightness values over homogeneous bottom types. If sea bottoms are not uniform, the transformed brightness values derived from principal components analysis are regressed against known depths for each type (Mishra *et al*., 2004). Once the model is constructed *via* regression analysis using a portion of the *in situ* sea water truth data, it can be validated using the remaining samples. A root-mean-square (RMS) error is generated to indicate the model accuracy.

3 Sensible depth
The sensible depth using the optical method varies with a number of factors. Theoretically, the 0.48–0.60 µm radiation is able to penetrate clear, calm ocean water by up to 15–20 m. The detectable depth has been reported at various levels. Passive optical systems have a limited depth penetration which is generally no better than 1.5 Secchi depths. The correlation is noticeably close at a shallower depth, with the best detectability occurring at approximately 10 m (Bagheri *et al*., 1998). Bottom depth and features appear to be observable down to 3–20 m, dependent on the water composition and bottom type (Spitzer and Dirks, 1986). However, the calculated penetration depth as obtained from the least-squares fit is about 37 m from MSS band 4 in Penang Island of Malaysia (Ibrahim and Cracknell, 1990). From band 4 (0.77–0.80 µm) of IRS LISS-II data, a deeper navigational route with a depth range of 8±10 m was identifiable, together with shoaling areas less than 5 m deep (Kumar *et al*., 1997). Coastal bathymetry can

be adequately detected from the Airborne Visible-Infrared Imaging Spectrometer data over the 10–15.5 m depth range (McIntyre *et al*., 2006).

As implied above, the sensible depth is affected by the wavelength of the solar radiation used and by water clarity. Water depth exerts a variable influence on remote sensing of bathymetry. It affects not only bottom reflectance but also the accuracy of the sensed bathymetry. The influence of this factor will be discussed below.

V Mapping accuracy and contributing factors
The accuracy of the retrieved water depth is subject to the influence of the sensing environments (eg, solar elevation and azimuth, platform height), atmospheric absorption and scattering, water surface conditions (eg, roughness, waves and currents), scattering by in-water constituents, and substrate reflectance properties that might affect the characteristics of the returned electromagnetic radiation. In addition to image properties, the accuracy of remotely sensing bathymetry is affected by a variety of water-related factors, such as water clarity, attenuation, depth, bottom reflectance if present, and bottom materials. The retrieved bathymetry may be made more accurate by considering a number of relevant factors. For instance, errors are reduced considerably after correction for the solar and view-angle effects (Lyzenga *et al*., 2006). Mapping can also be made more accurate by taking into account water quality and bottom reflectance.

1 Accuracy
Accuracy of bathymetric retrieval using the optical method is usually expressed *via* the R^2 value of the regression model. Regression of observed water depth against TM2 and MSS1 typically yield an r value of about 0.7 and 0.62, respectively (Baban, 1993). A site-specific relationship derived from spectral ratios of remote sensing reflectance achieved nearly perfect accuracy of R^2=0.97

in mapping bathymetry to the metre-scale resolution (Dierssen *et al*., 2003). Estimation error appears to increase with water depth with the estimates being accurate for water depth up to 7.5 m. In terms of RMS errors, bathymetric information derived from IKONOS imagery in combination with a tide chart has an accuracy of 0.87 m (Muslim and Foody, 2008). The modelled water depth has an RMS error of 7.83%, with the depth most accurate over the range of 10–14 m (McIntyre *et al*., 2006). A bathymetric map derived from SPOT images has a mean difference of about 20% from *in situ* measured depths (Lafon *et al*., 2002). Lyzenga *et al*. (2006) achieved an aggregate RMS error of 2.3 m from a set of IKONOS images over a variety of conditions. The individual RMS error varied from 1.65 to 2.31 m. The high accuracy is attributed to the physically based model that takes into account a number of factors, and the use of fine-resolution IKONOS images. In bathymetric mapping, the most accurate results reported so far have a standard error of 0.648 m (Mishra *et al*., 2004).

The accuracy of optically sensing bathymetry is subject to image spatial, spectral, and radiometric resolutions that may have a confounding effect. The spatial resolution of early systems is too coarse for bathymetric mapping, especially over shallow estuarine environments. Contemporary sensing systems such as IKONOS (having a spatial resolution measured in metres) hold great potential for the derivation of accurate bathymetric data. Regression of logged depth against IKONOS bands yielded an R^2 value over 0.87 (Muslim and Foody, 2008), much higher than the maximum R^2 value of only 0.35 achieved from MSS and TM bands of 30–79 m resolution (Baban, 1993). This suggests that a finer spatial resolution is conducive to more accurate bathymetric information. On the other hand, the inverse depth had a correlation coefficient of 0.56 with TM band 1 (30 m resolution), but only 0.51 with SPOT XL band 1 (20 m resolution;

Ji *et al*., 1992). The best results obtained from the Geophysical Environmental Research Hyperspectral Imaging Spectrometer data have an r of 0.974 with water depth, highly similar to simulated Landsat TM (r = 0.964) (Bagheri *et al*., 1998). Thus, a fine spectral resolution is not always critical in generating highly accurate bathymetric information. Instead, radiometric resolution is at least as important as hyperspectral selectivity for bathymetric applications under the attending conditions.

2 Impact of water turbidity

Water turbidity is the most important factor affecting the accuracy of optically sensed bathymetry. Turbidity obstructs the path of electromagnetic radiation, and reflectance from suspended particles becomes confused with bottom reflectance. Waters of different turbidity levels scatter the incoming radiation differently. Both the form and accuracy of the empirical model in equation (6) are affected by water turbidity that exerts a varying impact on the accuracy and depth of remotely sensed bathymetry. On the one hand, it enables sensing of depth in highly turbid Case II waters. On the other, it considerably lowers the detectable water depth. The regression relationship varies slightly with water clarity (Lafon *et al*., 2002). Thus, the same regression model established from turbid waters cannot be applied to clear waters. If calibrated with *in situ* measurements, remote sensing reflectance enables the retrieval of water depth up to 6 m in Case II water, and for total suspended matter concentrations ranging from 0.2 to 9 mg l^{-1}. In fact, if water turbidity is rather low (eg, clear water), the results could be encouraging from TM data (Cracknell *et al*., 1987). If the water has too high a turbidity, the sensible depth will be drastically reduced. The depth of highly turbid water is difficult to determine by the optical bathymetry method (Tripathi and Rao, 2002).

The influence of turbidity on depth measurements can be compensated for by applying

a correction factor to the reflectance (Tripathi and Rao, 2002). Since a higher concentration of suspended sediment concentration (SSC) level causes stronger backscattering of the incident light from the water (Yoshino and Yoshitani, 1988) and hence a larger pixel value, the influence of SSC should be negated by dividing the reflectance in a spectral band by the concentration level, or:

$$D = A + B\frac{R}{SSC} \qquad (7)$$

The above modification is acceptable if SSC is vertically uniform. If not, some kind of averaging over the water column should be undertaken first to ensure the highest accuracy of modelling.

3 Impact of water depth

Bottom reflectance is the reflectance from the sea floor that is not indicative of water depth directly. It occurs in shallow waters or in relatively deep clear water when the solar radiation is able to penetrate the water column to reach the floor. The exact depth at which bottom reflectance ceases, however, is a function of the in-water constituents and the sensing wavelength. Depth-independent bottom reflectance can be retrieved from remote sensing reflectance using bathymetry and tables of modelled water column attenuation coefficients (Lafon *et al.*, 1997).

Bottom reflectance is a major factor in comparison with water column scattering in the radiance emergent from water in very shallow and turbid waters. This enables the development of a water column scattering-based remote bathymetric model which can be applied to turbid and deeper coastal waters (Ji *et al.*, 1992). Bottom reflectance must be factored in by radiometrically modifying the reflectance prior to regression analysis. Bottom reflectance is related to bottom type. The regression coefficients deteriorate with mixed bottom types because the variability in brightness values from a heterogeneous bottom has a deleterious effect on the correlation coefficient. A uniform type

of bottom reduces this variability and leads to a strong correlation between depth and brightness value, thus improving the accuracy of estimated depths (Mishra *et al.*, 2004). In order to guarantee the validity and accuracy of equation (6), it is imperative that separate models be constructed for differing types of floor material.

The best way of handling bottom reflectance is to measure it and then subtract this from the total reflectance if the water is sufficiently clear. More precise processing involves retrieving depth-independent bottom reflectance from the sensed reflectance using bathymetry and tables of modelled water column attenuation coefficients (Dierssen *et al.*, 2003). Otherwise, a scattering coefficient needs to be applied. One method of ascertaining the relative substrate reflectance is to unmix the exponential influence of depth in each pixel of multi-spectral imagery under a mathematical constraint (Bierwirth *et al.*, 1993). Derivation of bathymetry from multi-spectral data is problematic if the substrate reflectance varies appreciably (Nordman *et al.*, 1990). This requires the removal of the distorting influence of the water column on the remotely sensed signal with the assistance of the mechanistic radiative transfer approach (Dierssen *et al.*, 2003). The superimposition of substrate reflectance from multi-spectral bands allows the distinction of different bottom materials.

VI Summary and conclusions

There are two broad types of methods used in the remote sensing of bathymetry: active non-imaging LiDAR and passive optical imaging. The former method is able to detect spot heights at sensed points, but this method did not find wide applications until recently due to technical constraints of low sampling density and slow scanning. The successful overcoming of these limitations, in conjunction with the use of kinematic GPS, has considerably increased the popularity of this method. This method has the advantage of being able to detect a large range of depths

up to 70 m in clear open waters at an accuracy close to 15 cm. However, as an airborne system, LiDAR is suitable for bathymetric mapping only over relatively small areas. This limitation will disappear once space-borne LiDAR systems become available. LiDAR is able to generate accurate bathymetric spot data quickly without the need for concurrent depth samples, but the data may be expensive and too coarse for precise applications. LiDAR accuracy and applicability is additionally constrained by water turbidity.

By comparison, the passive optical imaging method is more flexible, in that it can be implemented either analytically or empirically. Analytical modelling is based on the physics of light transmission within a water body. This implementation is theoretically sound, but is hampered by its complexity, since it requires the input of *in situ* measured parameters relating to the optical properties of water and the floor material. Empirical modelling is much easier to implement, since it requires only a limited number of *in situ* measurements at certain sampling spots to build a relationship between bathymetry and image properties. Linear or non-linear regression relationships between the two variables are, at least partially, able to take the ambient sensing environment into account. This implementation may produce results which have similar accuracy to the analytical or semi-analytical implementations under certain circumstances. The passive imaging method is widely applicable to both shallow turbid coastal waters, estuaries, inland lakes, and even open oceanic waters. A huge area can be mapped very quickly at a fine spatial resolution. At a typical depth of up to 20 m, this method has a much weaker bathymetric detection capability than the LiDAR method, however, and it is critically limited by the requirement for concurrently measured sea-truth data at the time of imaging. The achievable accuracy of detection varies, but is markedly lowered at deeper depths, in turbid coastal waters and where bottom materials vary.

References

Aarninkhof, S.G.J., Ruessink, B.G. and Roelvink, J.A. 2005: Nearshore subtidal bathymetry from time-exposure video images. *Journal of Geophysical Research C: Oceans* 110, 1–13.

Aarninkhof, S.G.J., Turner, I.L., Dronkers, T.D.T., Caljouw, M. and Nipius, L. 2003: *Coastal Engineering* 49, 275–89.

Abbot, R.H., Lane, D.W., Sinclair, M. J. and Spruing, T.A. 1996: Lasers chart the waters of Australia's Great Barrier Reef. *Proceedings of the Society of Photographic Instrumentation Engineers* 2964, 72–90.

Baban, S.M.J. 1993: The evaluation of different algorithms for bathymetric charting of lakes using Landsat imagery. *International Journal of Remote Sensing* 14, 2263–73.

Bagheri, S., Stein, M. and Dios, R. 1998: Utility of hyperspectral data for bathymetric mapping in a turbid estuary. *International Journal of Remote Sensing* 19, 1179–88.

Benny, A.H. and Dawson, G.J. 1983: Satellite imagery as an aid to bathymetric charting in the Red Sea. *The Cartographic Journal* 20, 5–16.

Bierwirth, P.N., Lee, T.J. and Burne, R.V. 1993: Shallow sea-floor reflectance and water depth derived by unmixing multispectral imagery. *Photogrammetric Engineering and Remote Sensing* 59, 331–38.

Calkoen, C.J., Hesselmans, G.H.F.M., Wensink, G.J. and Vogelzang, J. 2001: The Bathymetry Assessment System: efficient depth mapping in shallow seas using radar images. *International Journal of Remote Sensing* 22, 2973–98.

Cracknell, A.P., Ibrahim, M. and McManus, J. 1987: Use of satellite and aircraft data for bathymetry studies. Advances in digital image processing. In *Proceedings of the RSS 13th Annual Conference, Nottingham*, Remote Sensing Society, University of Nottingham, 391–402.

Dierssen, H.M., Zimmerman, R.C., Leathers, R.A., Downes, T.V. and Davis, C.O. 2003: Ocean color remote sensing of seagrass and bathymetry in the Bahamas Banks by high-resolution airborne imagery. *Limnology and Oceanography* 48, 444–55.

Finkl, C.W., Benedet, L. and Andrews, J.L. 2005: Submarine geomorphology of the continental shelf off southeast Florida based on interpretation of airborne laser bathymetry. *Journal of Coastal Research* 21, 1178–90.

Fonstad, M.A. and Marcus, W.A. 2005: Remote sensing of stream depths with hydraulically assisted bathymetry (HAB) models. *Geomorphology* 72, 320–39.

George, D.G. 1997: Bathymetric mapping using a compact airborne spectrographic imager (CASI). *International Journal of Remote Sensing* 18, 2067–71.

Guenther, G.C., Brooks, M.W. and **Larocque, P.E.** 2000: New capabilities of the 'SHOALS' airborne lidar bathymeter. *Remote Sensing of Environment* 73, 247–55.

Hickman, G.D. and **Hogg, J.E.** 1969: Application of an airborne pulsed laser for near shore bathymetric measurements. *Remote Sensing of Environment* 1, 47–58.

Ibrahim, M. and **Cracknell, A.P.** 1990: Bathymetry using Landsat MSS data of Penang Island in Malaysia. *International Journal of Remote Sensing* 11, 557–59.

Ji, W., Civco, D.L. and **Kennard, W.C.** 1992: Satellite remote bathymetry: a new mechanisms for modeling. *Photogrammetric Engineering and Remote Sensing* 58, 545–49.

Kumar, V.K., Palit, A. and **Bhan, S.K.** 1997: Bathymetric mapping in Rupnarayan–Hooghly river confluence using IRS data. *International Journal of Remote Sensing* 18, 2269–70.

Lafon, V., Froidefond, J.M. and **Castaing, P.** 1997: Bathymetric mapping by SPOT images to quantify sand movements in the tidal inlet of Arcachon (France). Earth Surface Sensing. Proc. SPIE conference, London, 456–66.

Lafon, V., Froidefond, J.M., Lahet, F. and **Castaing, P.** 2002: SPOT shallow water bathymetry of a moderately turbid tidal inlet based on field measurements. *Remote Sensing of Environment* 81, 136–48.

Lyzenga, D.R. 1978: Passive remote sensing techniques for mapping water depth and bottom features. *Applied Optics* 17, 379–83.

— 1985: Shallow-water bathymetry using combined lidar and passive multispectral scanner data (Bahama Islands). *International Journal of Remote Sensing* 6, 115–25.

Lyzenga, D.R., Malinas, N.P. and **Tanis, F.J.** 2006: Multispectral bathymetry using a simple physically based algorithm. *IEEE Transactions on Geoscience and Remote Sensing* 44, 2251–59.

Mallet, C. and **Bretar, F.** 2009: Full-waveform topographic lidar: state-of-the-art. *ISPRS Journal of Photogrammetry and Remote Sensing* 64, 1–16.

McIntyre, M.L., Naar, D.F., Carder, K.L., Donahue, B.T. and **Mallison, D.J.** 2006: Coastal bathymetry from hyperspectral remote sensing data: comparisons with high resolution multibeam bathymetry. *Marine Geophysical Researches* 27, 128–36.

Mishra, D., Narumalani, S., Lawson, M. and **Rundquist, D.** 2004: Bathymetric mapping using IKONOS multispectral data. *GIScience and Remote Sensing* 41, 301–21.

Muirhead, K. and **Cracknell, A.P.** 1986: Airborne lidar bathymetry. *International Journal of Remote Sensing* 7, 597–614.

Muslim, A.M. and **Foody, G.M.** 2008: DEM and bathymetry estimation for mapping a tide-coordinated shoreline from fine spatial resolution satellite sensor imagery. *International Journal of Remote Sensing* 29, 4515–36.

Nordman, M.E., Wood, L., Michalek, J.L. and **Christy, J.L.** 1990: Water depth extraction from Landsat-5 imagery. In *Proceedings of the Twenty-third International Symposium on Remote Sensing of Environment*, 1129–39.

Philpot, W.D. 1989: Bathymetric mapping with passive multispectral imagery. *Applied Optics* 28, 1569–78.

Polcyn, F.C. and **Lyzenga, D.R.** 1979: Landsat bathymetric mapping by multispectral processing. In *Proceedings of the Thirteenth International Symposium on Remote Sensing of Environment*, Ann Arbor, MI: International Society for Photogrammetry and Remote Sensing (ISPRS), 1269–76.

Roberts, A.C.B. and **Anderson, J.M.** 1999: Shallow water bathymetry using integrated airborne multispectral remote sensing. *International Journal of Remote Sensing* 20, 497–510.

Sichoix, L. and **Bonneville, A.** 1996: Prediction of bathymetry in French Polynesia constrained by shipboard data. *Geophysical Research Letters* 23, 2469–72.

Siegal, B.S. and **Gillespie, A.R.** 1980: *Remote sensing in geology*. New York: Wiley.

Spitzer, D. and **Dirks, R.W.J.** 1986: Classification of bottom composition and bathymetry of shallow waters by passive remote sensing. Remote sensing for resources development and environmental management. In *Proceedings of the 7th ISPRS Commission VII Symposium, Enschede*, volume 2, 775–77.

Tripathi, N.K. and **Rao, A.M.** 2002: Bathymetric mapping in Kakinada Bay, India, using IRS-1D LISS-III data. *International Journal of Remote Sensing* 23, 1013–25.

Tronvig, K.A. 2005: Near-shore bathymetry. *Hydro International* 9, 24–25.

Vogelzang, J., Wensink, G.J., de Loop, G.P., Peters, H.C. and **Pouwels, H.** 1992: Sea bottom topography with X-band SLAR: the relation between radar imagery and bathymetry. *International Journal of Remote Sensing* 13, 1943–58.

Wang, C.-K. and **Philpot, W.D.** 2007. Using airborne bathymetric lidar to detect bottom type variation in shallow waters. *Remote Sensing of Environment* 106, 123–35.

Warne, D.K. 1972: Landsat as an aid in the preparation of hydrographic charts. *Photogrammetric Engineering and Remote Sensing* 44, 1011–16.

Yoshino, F. and **Yoshitani, J.** 1988: Water depth estimation based on attenuation and bottom reflectance. In *Proceedings of the Ninth Asian Conference on Remote Sensing, Bangkok, Thailand*, Asian Association of Remote Sensing, University of Tokyo, F-9-1–8.